Physics Letters B 740 (2015) 8–15

Contents lists available at ScienceDirect

Physics Letters B

www.elsevier.com/locate/physletb

Effective theories and measurements at colliders

Christoph Englert [a,*], Michael Spannowsky [b]

[a] SUPA, School of Physics and Astronomy, University of Glasgow, Glasgow, G12 8QQ, United Kingdom
[b] Institute for Particle Physics Phenomenology, Department of Physics, Durham University, DH1 3LE, United Kingdom

ARTICLE INFO

Article history:
Received 4 September 2014
Received in revised form 3 November 2014
Accepted 17 November 2014
Available online 20 November 2014
Editor: A. Ringwald

ABSTRACT

If the LHC run 2 will not provide conclusive hints for new resonant Physics beyond the Standard Model, dedicated and consistent search strategies at high momentum transfers will become the focus of searches for anticipated deviations from the Standard Model expectation. We discuss the phenomenological importance of QCD and electroweak corrections in bounding higher dimensional operators when analysing energy-dependent differential distributions. In particular, we study the impact of RGE-induced operator running and mixing effects on measurements performed in the context of an Effective Field Theory extension of the SM. Furthermore, we outline a general analysis strategy which allows a RGE-improved formulation of constraints free of theoretical shortcomings that can arise when differential distributions start to probe the new interaction scale. We compare the numerical importance of such a programme against the standard analysis approach which is widely pursued at present.

1. Introduction

After the Higgs discovery in 2012 [1,2], the ATLAS and CMS Collaborations have started to investigate the new particle's properties in further detail [3]. For run 1, the Higgs boson's couplings have been constrained primarily using ratios

$$\kappa = (g_{\rm SM} + \Delta g_{\rm BSM})/g_{\rm SM} \tag{1}$$

see Ref. [4] for details. These quantities are inclusive with respect to the phase space and are determined by comparing the number of measured events with the Standard Model prediction after subtracting the background for a given process. While this strategy is a reasonable procedure to obtain limits with relatively small statistics and large systematic uncertainties, a larger parameter space will become accessible during run 2, and a more fine-grained picture of constraints on interactions beyond the SM (BSM) can be formulated at higher LHC luminosity and energy.

In the absence of new resonant effects, a common approach to parametrise new physics interactions is to employ effective theory methods [5–8]. Imposing simplifying assumptions, such as *e.g.* the absence of non-trivial BSM flavour structures, one obtains a basis of 59 independent operators that express our lack of knowledge of the underlying new physics model at a high scale [7].

New physics at energy scales larger than the electroweak scale will typically show up as modifications of differential distributions at high transverse momenta. While an increased cross section can be observable in inclusive "$\sigma \times$ BR physics", a proper investigation of differential distributions is not only far more adequate to this particular physics question, but will also provide significantly more insight into the nature of BSM physics if a significant excess over the SM will be observed eventually.

A clear advantage of abandoning the κ prescription of Eq. (1) in favour of an effective field theory approach with a general set of Higgs interaction operators is that information from differential distributions does have a theoretically meaningful interpretation. The presence of dimension 6 operators will not only alter the total rate, but also the shape of measured distributions and new physics searches (in the absence of new kinematically accessible resonances) can be studied in a fairly model-independent way.

However, there are a few caveats. Using differential distributions can also mean a challenge for the effective theory approach. Effective theory, being an expansion in a new physics interaction scale $\Lambda_{\rm NP}$, is strictly speaking only valid when typical interaction scales are distinctively separated, *i.e.* when we have $\Lambda_{\rm NP} \gg \Lambda_{\rm interaction}$ for all relevant scales of the considered process. A well-known example for this is flavour physics, where effective field theories have always been an important tool. When studying rare decays, the weak interaction scale $\Lambda_{\rm NP} = m_W$ is clearly separated from the scale at which B-Mesons decay $\Lambda_{\rm interaction} = m_b$, which acts as the characteristic measurement scale. Corrections

* Corresponding author.
E-mail addresses: christoph.englert@glasgow.ac.uk (C. Englert), michael.spannowsky@durham.ac.uk (M. Spannowsky).

http://dx.doi.org/10.1016/j.physletb.2014.11.035

to the effective theory description are parametrically suppressed by $\mathcal{O}(m_b^2/m_W^2) \sim 0.3\%$. Therefore, applying effective field theory methods provides a well-motivated and theoretically well-controlled approximation.

At collider experiments in general, but at hadron colliders in particular, it is challenging to infer the scale at which the effective operators are probed from the observed final state objects when we want to formulate a limit on the presence of new physics: Different events will always probe the theory prediction at different scales μ. For example, in mono-Higgs production where the Higgs recoils against a hard jet, the transverse momentum of the jet is a relevant scale at which the effective operator $\hat{H}^\dagger \hat{H} \hat{G}^{\mu\nu} \hat{G}_{\mu\nu}/\Lambda_{\rm NP}^2$ is probed.

On the one hand, a naive constraint on $C_O(v^2/\Lambda_{\rm NP}^2)$ can always be understood as a limit obtained with $\Lambda \ll \Lambda_{\rm NP}$ with an appropriate redefinition of the Wilson coefficient's size and we even might be tempted to lower $\Lambda_{\rm NP}$ to an energy range of a few TeV that is resolved by the LHC for an educated guess of the Wilson coefficient.[1] The reliability and robustness of such a limit is at least questionable as a naive analysis of a Wilson coefficient is performed completely independent of the matching or cut-off scale, which must not be kinematically resolved for the EFT expansion to hold in the first place.

On the other hand, if the effective Lagrangian is defined at a fixed scale $\Lambda_{\rm NP}$ *outside* the LHC reach or the observable's energy coverage,[2] or at least at the maximum energy probed in a new physics experiment with negative outcome, they mix when evolved from one scale to another as a consequence of electroweak and QCD interactions [10–12]. As a result, different phase space regions do probe different operator combinations. Thus, to infer well-defined constraints from exclusive distributions, the operators probed at different energy scales for different events or bins have to be evolved to a fixed predefined scale to allow a direct interpretation.

The impact of operator running is parametrically $\mathcal{O}(g_i \gamma_i \log[\Lambda_{\rm NP}/\Lambda_{\rm meas}])$, with coupling g_i and the anomalous dimension γ_i of the operator $\hat{O}_i$, the new physics scale $\Lambda_{\rm NP}$ and the measurement scale $\Lambda_{\rm meas}$. For B-decay observables with $\Lambda_{\rm NP} \simeq m_W$ and $\Lambda_{\rm meas} \simeq m_b$, the resummation of these large logarithms can provide an important theoretical improvement for the interpretation of the measurement. A priori, when studying Higgs boson properties and assuming no New Physics particles up to several TeV, the hierarchy of electroweak and New Physics scale (*e.g.* $\Lambda_{\rm NP} \simeq 2$ TeV) can be of similar order. Hence a resummation of these large logarithms can be crucial for a detailed understanding of the impact of Higgs-boson measurements on New Physics models.

In this paper, we study the impact of operator running and mixing on coupling measurements using differential distributions. We focus on three illustrative examples ranging from multi-jet to Higgs physics. To our knowledge these effects have not been discussed in a fully differential fashion at the LHC in the context of effective field theory measurements. We also provide a first step towards a general prescription of how measurements based on differential distributions can be used to constrain an effective Lagrangian, and how to give those constraints an interpretation in terms of a UV scale model, including higher-order corrections in a well-defined and practical way. As we will see, due to the momentum dependence of many of the higher-dimensional operators and their impact being most relevant when probed at large invariant masses, *i.e.* $\Lambda_{\rm meas} \simeq \sqrt{\hat{s}}$, the characteristic logarithms $\log(\Lambda_{\rm NP}/\sqrt{\hat{s}})$, depending on the assumed new physics scale $\Lambda_{\rm NP}$, are fairly small and the contributions of operator running is of $\lesssim$10%.

To make this work self-contained we review the (flavour physics) language relevant to this problem in Section 2 before we apply it to di-jet final states at the LHC. In Sections 5.1 and 5.2 we discuss the impact on Higgs phenomenology in $H+$jet and HZ production before we give our conclusions in Section 6.

2. Effective field theory approach: a quick review

In general an effective Hamiltonian in Operator Product Expansion is given by

$$\hat{\mathcal{H}}_{\rm eff} = \sum_i C_i(\mu)\hat{O}_i(\mu), \tag{2}$$

where $\hat{O}_i$ are the operators defined at the factorisation scale μ and C_i are the so-called Wilson coefficients. Note that as a consequence of factorisation, both the Wilson coefficient as well as the operators are scale-dependent. This dependence cancels for $\hat{\mathcal{H}}_{\rm eff}$. Eq. (2) separates the physics into a long-range behaviour of matrix elements $\langle \hat{O}(\mu)\rangle$ and short-range behaviour of Wilson coefficients $C_i(\mu)$ relative to the factorisation scale μ. The ignorance of physics with respect to this arbitrary separation at this stage leads to renormalisation group equations (RGEs). If we focus on a particular model, the coefficients of Eq. (2) can be obtained by a matching calculation. Only assuming SM particle content and gauge symmetries, the lowest order effective operator extension consists of dimension 6 operators documented in Ref. [7]. Relying on this language, we are fairly unprejudiced about the particular UV dynamics at a new physics scale $\Lambda_{\rm NP}$ (a well-motivated guess on the Wilson coefficients' hierarchies are possible when we consider composite Higgs scenarios [8]).

Approximating general amplitudes and eventually exclusive cross sections in terms of effective operators is only valid if the new physics scale $\Lambda_{\rm NP}$, the scale of the masses of the heavy degrees of freedom of the full theory, is much larger than the scale at which the effective operator is probed (see [13–16] for a discussion in the context of Higgs physics).

For example, in the Standard Model process $c\bar{s} \to u\bar{d}$ the leading-order amplitude is given by (we suppress the CKM matrix elements for convenience)

$$\begin{aligned}\mathcal{M} &= i\frac{G_F}{\sqrt{2}}\frac{M_W^2}{\hat{s}-M_W^2}(\bar{s}_a c_a)_{V-A}(\bar{u}_b d_b)_{V-A} \\ &= -i\frac{G_F}{\sqrt{2}}(\bar{s}_a c_a)_{V-A}(\bar{u}_b d_b)_{V-A} + \mathcal{O}\left(\frac{\hat{s}}{M_W^2}\right),\end{aligned} \tag{3}$$

assuming a diagonal CKM matrix and $(V-A)$ referring to the Lorentz structure $\gamma_\mu(1-\gamma_5)$ (we have made the colour indices a and b of the spinors explicit). Physics based on the effective operator $\hat{O}_2 = (\hat{\bar{s}}_a \hat{c}_a)_{V-A}(\hat{\bar{u}}_b \hat{d}_b)_{V-A}$ in Eq. (3) is clearly only valid for scales $\hat{s} = (p_{\bar{s}} + p_c)^2 \ll M_W^2$.

The EFT approach to matrix elements like Eq. (3) has been studied in detail and is well covered in flavor physics reviews and we refer the reader to [17] for details while we only quote the results in the following. The matching procedure at NLO QCD induces two operator structures

$$i\mathcal{M} = C_1\langle \hat{O}_1\rangle + C_2\langle \hat{O}_2\rangle. \tag{4}$$

As we perform a calculation in EFT with higher dimensional bare interactions $\sim C_i^{(0)}\hat{O}_i(\hat{\bar{u}}^{(0)}\hat{d}^{(0)}\hat{\bar{s}}^{(0)}\hat{c}^{(0)})$, there is an additional multiplicative renormalisation of the Wilson coefficients necessary

[1] This procedure has typically been applied in searches for Dark Matter at the LHC and has been left without criticism for quite some time [9].

[2] This situation is similar to electroweak fits after LEP2, which assumed a Higgs mass at the kinematic endpoint of $m_H \simeq 114$ GeV.

to arrive at the above result. This renormalisation implies the mentioned RGE for the Wilson coefficients

$$\frac{\mathrm{d}C_i}{\mathrm{d}\log\mu} = \gamma_{ij} C_j, \tag{5}$$

where the anomalous dimension matrix γ_{ij} is typically non-diagonal, hence leading to scale-dependent operator mixing under the RG flow. This evolution is entirely encoded in γ_{ij}.

The anomalous dimension is related to the multiplicative (counter term) renormalisation of the bare couplings $C^{(0)} = Z_C C = (1+\delta_C)C$,

$$\gamma = -\lim_{\varepsilon\to 0} \frac{\mathrm{d}\log Z_C}{\mathrm{d}\log\mu}, \tag{6}$$

in dimensional regularisation with $D = 4-2\varepsilon$. At the one loop level we can replace Z_C by the counter term δ_C for the Wilson coefficient. For the discussed case the anomalous dimension matrix reads

$$\gamma = \frac{1}{16\pi^2}\begin{bmatrix} -2g_s^2 & 6g_s^2 \\ 6g_s^2 & -2g_s^2 \end{bmatrix}. \tag{7}$$

3. Constraining new physics by measuring Wilson coefficients

In flavour physics, where this conceptual apparatus has been put to good use for the last decades [18], the lower characteristic scale usually corresponds to the mass of the decaying quark of the hadron whose properties are to be studied, *e.g.* $\hat{s} = m_b^2$. In contrast to that, at the LHC fixing the lower (IR) scale, *e.g.* $\hat{s} = m_H^2$, is not possible in all analyses. The range of $\hat{s}$ probed at the LHC, even for a single observable, can be large and extend easily to the multi-TeV regime as encountered in *e.g.* Higgs + jet phenomenology [19,20]. Therefore, due to operator running and mixing, each event probes a different combination of operators at $\hat{s}$. These measurements or constraints have to be related to the operators defined at the new physics scale Λ_{NP} to allow a consistent formulation of a combined constraint on a new physics model defined at this scale.

Being able to constrain or discover new physics contributions in differential distributions, *i.e.* measurements beyond total rates, is a particularly intriguing feature of the LHC with its large centre of mass energy and its increasing amount of integrated luminosity. During the upcoming runs at 13–14 TeV we can expect the focus of BSM searches to quickly move towards constraining EFTs with the help of differential distributions.

To ease the discussion of the examples of Sections 4–5.2 we give here a prescription of how to obtain constraints on new physics models in terms of effective theories at particle colliders, taking higher-order corrections and operator running into account:

The first step is of course to perform a measurement of the differential distributions relevant for the operators and processes at hand, *e.g.* m_{jj}, $\Delta\phi_{jj}$, $p_{T,l}$, y_b. An apt choice of the observable is crucial for the sensitivity of the analysis.

To constrain new physics models from the measured observables we add higher-dimensional operators, *e.g.* $\mathcal{L}_{\mathrm{dim6}}$, to the Lagrangian defined at a new physics scale Λ_{NP}. Differential distributions based on a calculation with the full $\mathcal{L} = \mathcal{L}_{\mathrm{dim4}} + \mathcal{L}_{\mathrm{dim6}}$ can now be compared to the measured differential distributions.

Obtaining and interpreting constraints on Wilson coefficients can be subtle:

(1) When calculating the theory prediction of the differential distribution we have to make sure that kinematic regions are avoided where the effective theory becomes invalid, *i.e.* we have to ensure that the effective operators are probed at energies below Λ_{NP} always. This can be achieved by studying the correlation of the measured distribution with the invariant mass $m_{\mathrm{inv}}^2 = (\sum_j p_j)^2$ of the external incoming or outgoing particles/fields present in the involved operator $\hat{O}_i$. We therefore suggest to record m_{inv} for every event studied, admittedly a task of varying complexity depending on the final state and the operators of interest. The maximum value of all recorded invariant masses $m_{\mathrm{inv}}^{\mathrm{max}}$ sets the lower cut-off for Λ_{NP} (the red horizontal line in Fig. 1), *i.e.* the lowest possible scale where the effective theory is well-defined. Depending on the size of the Wilson coefficient, the obtained limit can still be unphysical if unitarity is violated at scales lower than Λ_{NP}, which is an additional constraint that needs to be imposed [14]; this fact is reflected in Fig. 1 by a potentially smeared out region of where Λ_{NP} needs to be defined.

(2) After having fixed the upper scale where the effective theory is defined, it is worth noting that, because m_{inv} is different for each event, each measured (or binned) event probes a different combination of operators. Thus, for each measured event one has to relate the combination of operators at the measurement scale with the set of operators at Λ_{NP} by solving Eq. (5).

(3) After constraining the Wilson coefficients of an effective Lagrangian according to steps *1* and *2*, it is now possible to give an interpretation of the measurement in terms of new physics interactions. As the Wilson coefficients are always a combination of dimensionless couplings and powers of the new physics scale Λ_{NP}, *e.g.* for a dimension 6 operator $C_i\langle\hat{O}_i\rangle \sim g_{\mathrm{NP}}^2/\Lambda_{\mathrm{NP}}^2$, the constraint in the parameter space corresponds to a diagonal in the g_{NP}–Λ_{NP} plane, see Fig. 1. In other words, if the new physics scale is low, small couplings can be excluded by the measurement, thereby cutting deep into the parameter space of extensions of the Standard Model.

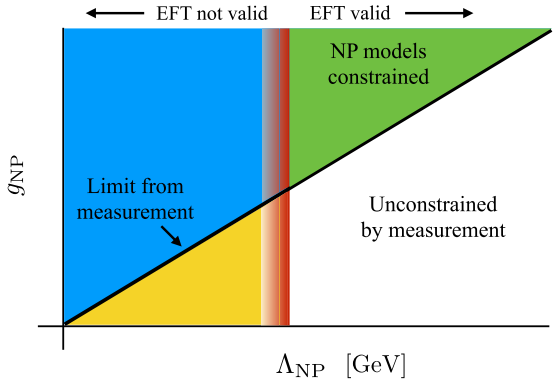

Fig. 1. New Physics interpretation of constraint on new operators $C(\Lambda_{\mathrm{NP}})\langle\hat{O}_{\mathrm{NP}}\rangle \sim (g_{\mathrm{NP}}/\Lambda_{\mathrm{NP}})^2$ (black line). The red vertical line indicates the validity cut-off of the effective theory. Only the parameter space captured the by green-shaded area is constrained using the effective theory approach. (For interpretation of the references to colour in this figure, the reader is referred to the web version of this article.)

Eventually, four sectors in the g_{NP}–Λ_{NP} plane can be identified, separated by the measured constraint on the Wilson coefficient (black line) and the threshold of the validity range of the effective theory (red line) in Fig. 1. *Both lines are inferred directly from the measurement*. The first sector in the upper left corner (blue shaded area) indicates that the measurement can rule-out small couplings, however this parameter choice is outside the validity range of the effective theory description, as is the yellow-shaded area (we could imagine a New Physics model with a resonance with smaller mass than Λ_{NP} to be in the BSM spectrum). The two sectors on the right

from the red line are within the validity range of the effective theory but only large couplings can be ruled out (green-shaded area). A large part of the parameter space is not constrained by the measurement (white-shaded area).

We note that our ignorance of physics at scales higher than the kinematic LHC cut-off for a given integrated luminosity needs to be strict in this picture. If we specify a model whose spectrum is resolved we can always define an effective theory at scales lower than the lowest new particle mass, but if this mass scale is resolved by the LHC, the only theoretically correct way to constrain models is to include the full model dependence on the propagating degrees of freedom. While the numerical effects can be small depending on the model, their full inclusion is well possible given the state-of-the-art of current Monte Carlo event generators.

4. Dijets and contact interactions at the LHC

Let us come back to the contact interaction model introduced in Section 2. To make our discussion transparent, we use these results for all contributing quark flavour-changing partonic subprocesses (and neglect the factor $G_F/\sqrt{2}$ in the operator definitions). We define the new physics scale and the resulting EFT at (i) $\Lambda_{\rm NP} = 14$ TeV, outside the kinematic LHC coverage of the run 2 start-up energy $\sqrt{s} = 13$ TeV and (ii) at the maximum energy of a low statistics phase during run 2 following Section 3 in a toy MC analysis. To take into account the operator mixing and to reflect the energy dependence of the Wilson coefficients when probed at different centre-of-mass energies $\sqrt{\hat{s}}$, we can solve the RGE resulting from Eqs. (5) and (7) and evaluate the effective Lagrangian at a specific energy scale on an event-by-event basis. Setting the correct scale at which we evaluate $\{C_i(\mu)\}$ involves some freedom, similar to choosing an appropriate scale, at which we evaluate the running of α_s in SM-like simulations of hadron collider processes. In this particular case we choose $\mu = \sqrt{\hat{s}}$, which is also chosen to be the relevant scale for parton densities and the running of the strong coupling.

In Fig. 2 we display the differential impact of taking into account the RGE-improved separation of $\Lambda_{\rm NP} = 14$ TeV from the scale at which the effective Lagrangian is probed as a function of the jets' transverse momentum $p_{T,j}$.[3]

Generally the absolute effects dominated over the RGE improved event simulation as becomes obvious from the logarithmic plot in Fig. 2. The induced relative difference turns out to be of order $O(10\%)$ in this particular example. Depending on the size of the data sample and the systematic uncertainty this could in principle be the level at which the LHC will be able to probe jet distributions at large luminosities during run 2.

Obviously, for our choice of $\Lambda_{\rm NP}$, the impact of RGE effects are not very large and will not account for the dominant uncertainties on non-standard interactions at the beginning of run 2 (see Refs. [24,25] for a discussion of systematic uncertainties of jet measurements at the LHC). Given the 10% relative impact of a theoretically clean separation of new physics and measurement scale as demonstrated in Fig. 2, we can turn the argument around to validate the practitioner's approach of setting limits on the presence of the new operators without taking into account the running of RGEs, since their numerical impact is not too large.

The latter point is demonstrated in Fig. 3. There we show a scan of the jet p_T distribution in a toy analysis to set constraints for

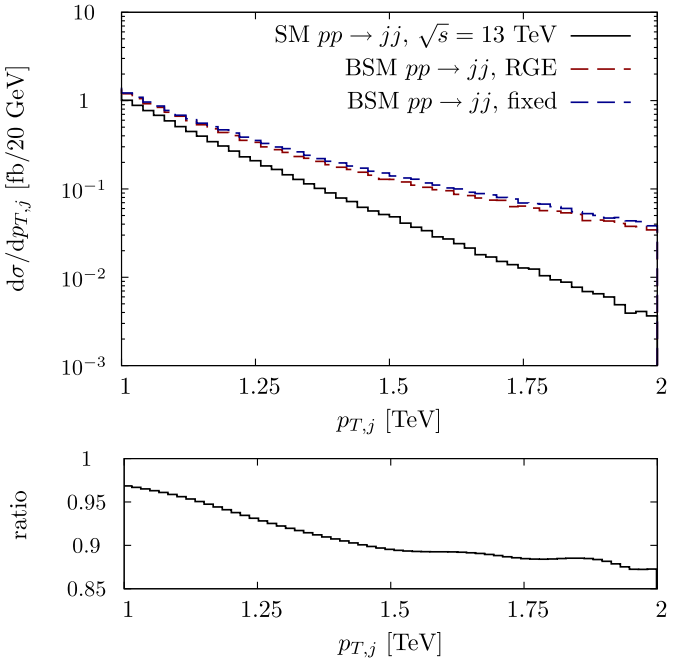

Fig. 2. Transverse momentum distribution of dijet events at the LHC with $\sqrt{s} = 13$ TeV. We show the SM and two scenarios including the effective operators of Section 2. Scenario 1 (2) refers to a choice of the Wilson coefficient of $C_1 = C_2 = 10$. "fixed" refers to the non-RGE improved distributions and "RGE" refers to distributions obtained by fixing the effective Lagrangian at $\Lambda = 14$ TeV and using the RGEs to consistently resum QCD effects to the measurement scale $\sqrt{\hat{s}}$. The ratio panel gives the differential impact of including the RGE running, displaying the ratio of "fixed" and "RGE".

new physics effects. Neglecting intricate and sophisticated experimental techniques to set limits we consider a parameter point in the (C_1, C_2) as constrained when a bin in the differential distribution depart from the SM hypothesis by 3σ at $\mathcal{L} = 1/\text{fb}$. We thereby constrain the "fixed" distribution of Fig. 2 at a certain scale μ; this yields the yellow box exclusion contour as indicated in Fig. 3. The overlayed contour indicated by the crosses shows how the former contour will be modified if we solve the RGEs upon inputting the differential measurement. While the overall modifications can be quite significant, the relative shape between the two choices of $\Lambda_{\rm NP}$ is small. Since dijet production has a large cross section we start to explore the tail of the distribution very early on during run 2.

5. Applications to Higgs phenomenology

5.1. Impact of operator running: Higgs + jet searches

As a first application to Higgs physics and to get an idea of the typical size of the RGE effects for Higgs phenomenology, we discuss the impact of operator running on Higgs + jet production [19,20]. Higgs + jet production is highly relevant for $H \to$ invisible [26] and the measurement of Higgs couplings in the SM and beyond [20]. While the former scenarios involve new degrees of freedom at low energy scales, it can be expected that "genuine" modifications of Higgs physics result from new dynamics at scales much higher than the electroweak scale. In fact, if we interpret the Higgs boson as a pseudo Nambu–Goldstone boson following [8], the new physics scale can easily be pushed to the multi-TeV regime or even beyond the kinematic LHC coverage if we admit some degree of fine-tuning. Strong interactions-induced deviations from the SM Higgs phenomenology will be associated with new resonant phenomena at the compositeness scale in these scenarios.

[3] These results have been obtained with a modified version of MadEvent/MadGraph v5 [21], inputting a UFO [22] model file generated with FEYNRULES [23]. We select jets in $|\eta_j| \leq 2.5$ using the Monte Carlo's default settings. The toy model could be thought of in terms of an already constrained very massive W' boson. We have checked that an analogous Z' model leads to similar results.

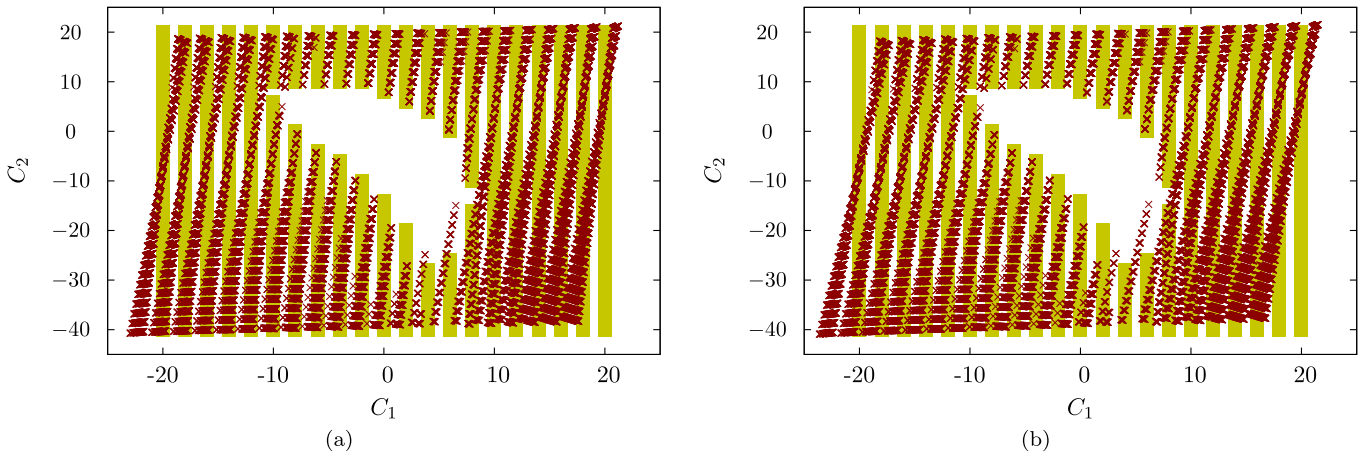

Fig. 3. Result of the limit setting analysis as detailed in the text. Excluded regions are indicated by boxes (not including RGE running) and crosses (including the RGE evolution to a common scale set by the maximum scale probed in a toy Monte Carlo analysis of a sample of $\mathcal{L} = 1/\text{fb}$, $\Lambda_{\text{NP}} \simeq 8$ TeV (a) and outside the run 2 energy coverage $\Lambda_{\text{NP}} = 14$ TeV (b)). To allow for direct a comparison we rescale the Wilson coefficients by $[14\ \text{TeV}/\max m_{\text{inv}}]^2$ for (a).

In the following we will again assume that those states are outside the direct sensitivity range of the LHC by defining $\Lambda_{\text{NP}} = 14$ TeV.

The $pp \to H +$ jet cross section receives modifications from a modified Yukawa and effective ggH sector [19,20]. To keep our discussion transparent at this stage we only focus on the latter operator in the following (*i.e.* we choose like Yukawa interaction $m_t = y_t v/\sqrt{2}$); to leading logarithmic approximation the two effective operator contributions are decoupled and the effective ggH sector

$$\hat{O}_G = \frac{g_s^2}{2\Lambda_{\text{NP}}^2} \hat{H}^\dagger \hat{H} \hat{G}^a_{\mu\nu} \hat{G}^{a\mu\nu} \tag{8}$$

gives rise to a form-invariant class of new interactions under RGEs (we will study the impact of running-induced operator mixing for the more interesting case of associated Higgs production in the subsequent section).

The anomalous dimension has been presented in [10]

$$\gamma_G = \frac{1}{16\pi^2}\left(-\frac{3}{2}g'^2 - \frac{9}{2}g^2 + 12\lambda + 6y_t^2\right), \tag{9}$$

where the authors have used the background field method (note that we assume a dominant top quark contribution to the Higgs wave function renormalisation in the following). λ denotes the Higgs self-coupling $V(H^\dagger H) \supset \lambda (H^\dagger H)^2$.

We have validated this result against an independent calculation in general R_ξ gauge [28] using the FeynRules [23] and FeynArts/FormCalc [27] packages. Note that due to the combination of couplings and gluon field strength tensors in Eq. (8), the anomalous dimension has no dependence on the strong coupling. This is obvious in the background field method [10] but non-trivial in R_ξ gauge. To obtain the result of Eq. (9) we perform a $\overline{\text{MS}}$ renormalisation of the Higgs and gluon wave functions, as well as of the strong coupling g_s.

Analogous to our discussion in Section 4 we show the impact of the running for two scenarios that correspond to two choices of Wilson coefficients

$$\text{Scenario 1:} \quad C_g = 10, \tag{10}$$

$$\text{Scenario 2:} \quad C_g = 100, \tag{11}$$

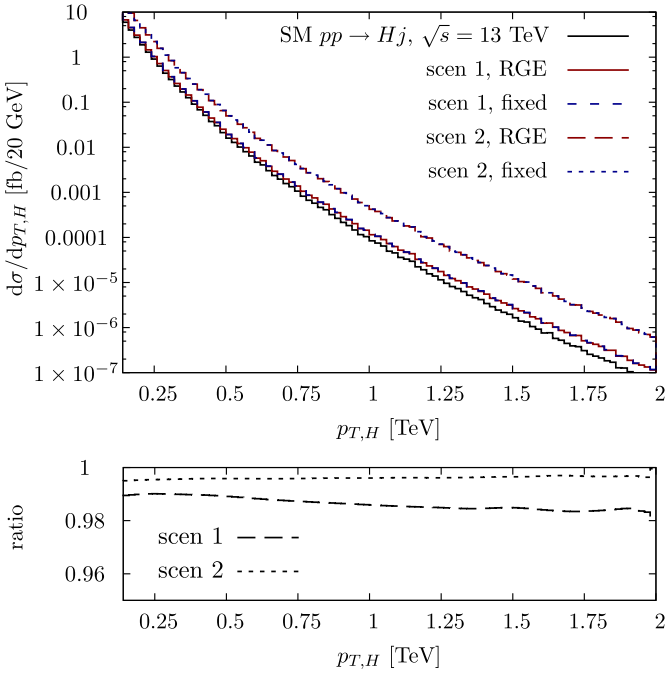

Fig. 4. Transverse momentum of Higgs bosons produced in $pp \to H +$ jet production for two choices of the Wilson coefficients and $\Lambda_{\text{NP}} = 14$ TeV as detailed in the text. The lower panel shows the differential impact of the RGE running analogous to Fig. 2.

for $\Lambda_{\text{NP}} = 14$ TeV, and comparing the differential impact of the operator running in Fig. 4.[4] As it becomes obvious from Fig. 4 the RGE effects for $H +$ jet production are at the 1% level and therefore completely negligible in light of expected theoretical uncertainties in this channel [30]. Hence, the standard limit setting approach is sufficiently adequate.

5.2. Impact of operator running and mixing: Higgs associated production

The importance of operator running and mixing in separating IR effects at the electroweak scale from fundamental physics

[4] We use a purpose-built implementation of $pp \to H +$ jet based on the VBFNLO [29] framework that includes the full numerical solution of the RGE running resulting from Eq. (9). All relevant scales are chosen to be $\mu = p_{T,H} + m_H$.

at a scale $\Lambda_{\rm NP}$ has been discussed in the context of the Higgs branching ratio to photons and electroweak precision observables in [10,12].

A process that turns out to be seminal for the dimension 6 analysis of the Higgs sector is associated production $pp \to HZ$ [13,14,32,33]. Associated production has a relatively large cross section and it will typically be observed at high momentum transfers in boosted final states [31], where we can expect new operator contributions to be well-pronounced. This fact allows to access a plethora of new physics scenarios in a direct or indirect way [33].

For the sake of clarity we limit ourselves to quark-induced production and the closed set of operators under RGEs [10,11]

$$\hat{O}_W = \frac{g^2}{2\Lambda^2_{\rm NP}} \hat{H}^\dagger \hat{H} \hat{W}^a_{\mu\nu} \hat{W}^{a\mu\nu}, \tag{12}$$

$$\hat{O}_B = \frac{g'^2}{2\Lambda^2_{\rm NP}} \hat{H}^\dagger \hat{H} \hat{B}_{\mu\nu} \hat{B}^{\mu\nu}, \tag{13}$$

$$\hat{O}_{WB} = \frac{gg'}{\Lambda^2_{\rm NP}} \hat{H}^\dagger t^a \hat{H} \hat{W}^a_{\mu\nu} \hat{B}^{\mu\nu}, \tag{14}$$

where $t^a = \sigma^a/2$ are the generators of $SU(2)_L$, $\hat{W}^a_{\mu\nu}$, $\hat{B}_{\mu\nu}$ are the weak and hypercharge field strength tensor operators, respectively, with couplings g and g'.

The operators $\hat{O}_W$ and $\hat{O}_B$ renormalise the W^a and B field strengths, and $\hat{O}_{WB}$ measures the departure from tree-level custodial isospin (the ρ parameter) $m_W^2/m_Z^2 = \cos^2\theta_w + \mathcal{O}(v^4/\Lambda^2_{\rm NP})$. Hence, we can imagine valid models at intermediate scales, such as composite pseudo Nambu–Goldstone boson interpretations of the Higgs boson, to incorporate a hierarchy among the Wilson coefficients as discussed in *e.g.* Ref. [8].

Again, the anomalous dimension matrix was computed in Ref. [10]

$$\gamma_{WB} = \frac{1}{16\pi^2} \begin{bmatrix} \frac{1}{2}g'^2 - \frac{9}{2}g^2 + 12\lambda + 6y_t^2 & 0 & 3g^2 \\ 0 & -\frac{3}{2}g'^2 - \frac{5}{2}g^2 + 12\lambda + 6y_t^2 & g'^2 \\ 2g'^2 & 2g^2 & -\frac{1}{2}g'^2 + \frac{9}{2}g^2 + 4\lambda + 6y_t^2 \end{bmatrix}, \tag{15}$$

where we again assume top-Yukawa dominance and λ is the Higgs self-coupling $V(H^\dagger H) \supset \lambda (H^\dagger H)^2$. Again, we have validated this result against an independent calculation in general R_ξ gauge analogous to Section 5.1. In R_ξ gauge cancellations between the coupling and field strength renormalisation constants are non-trivial in the $\hat{O}_W$ and $\hat{O}_{WB}$ cases to yield the gauge-independent result of Eq. (15).

We study the impact of the RGE running for two scenarios fixing $\Lambda_{\rm NP} = 14$ TeV,

$$\text{Scenario 1:} \quad C_W, C_B = 0.25 \frac{v^2}{\Lambda^2_{\rm NP}}, \quad C_{WB} = C_{W,B}/(8\pi^2), \tag{16}$$

$$\text{Scenario 2:} \quad C_W, C_B \simeq 0.50 \frac{v^2}{\Lambda^2_{\rm NP}}, \quad C_{WB} = C_{W,B}/(8\pi^2). \tag{17}$$

which reflects a UV hierarchy to provide and acceptable ρ parameter following [8].

The results are shown in Fig. 5.[5] Again the impact of RGE running can be of the order of $\lesssim$10% in the boosted cut threshold regime where this process can be isolated from the background [31] and be used to constrain new interactions [33]. There is a mild dependence of the RGE corrections on the size of the input Wilson coefficient and due to the particular slope that results from Eq. (9) the deviations become relevant at low scales where we can expect the statistical und systematic uncertainties to become small compared to the p_T distribution's tail eventually. The ratio quickly converges to one for scales probing $\mathcal{O}$ (TeV) scales. Therefore, for large luminosities, the separation effects of $\mu \ll \Lambda_{\rm NP}$ might be relevant when we will try to pin down Higgs coupling properties at the 10% level.

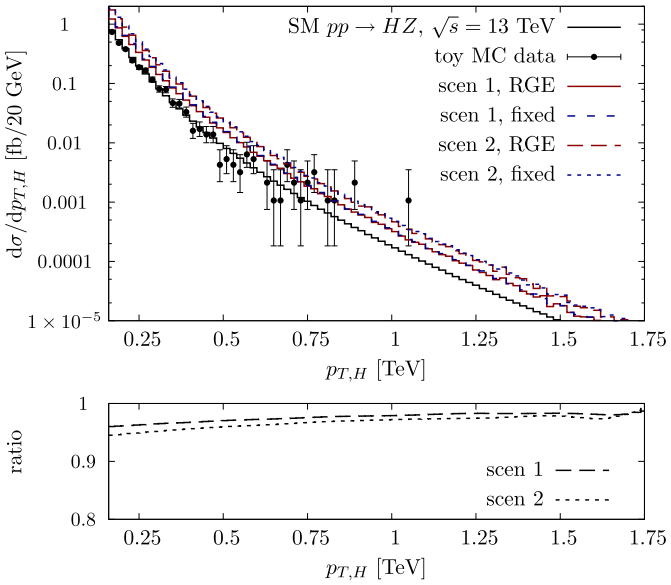

Fig. 5. Transverse momentum distribution of the Higgs boson in the high p_T regime relevant to boosted analyses [31] including a toy Monte Carlo data sample (for details see text). We show two scenarios referring to different choices of the Wilson coefficients that are mixed under the RGE flow.

5.3. Interplay between measurement and interpretation in Higgs associated production

We will use the example of associated production to follow the description of Section 3 more closely. We investigate the impact on the expected limits numerically with the aim to establish a connection between measurement, RGE running and the interpretation of the measurement of in terms of a UV theory.

The first step is to perform a measurement with a given data set, that determines a maximally resolved scale that probes the operators in the limit setting exercise. We do this by generating an unweighted SM event sample of a given luminosity which allows to determine the maximum $m_{\rm inv}$ by reconstructing the final state. As we have discussed in Section 3, $C_i \langle \hat{O}_i \rangle \sim g_i^2/\Lambda^2_{\rm NP}$, and by identifying $\Lambda \simeq m_{\rm inv}^{\rm max}$ we assume that the new resonances of the UV theory are not yet probed with this data set.[6] At the same time, however, we can answer the question of what is the smallest coupling of the UV theory that we can constrain or exclude in the light of the measurement (if we deal with a well-defined UV model we can alternatively rephrase this in terms of a lower bound on the involved mass scales). This is usually a question of interest: How far into the parameter space of the UV theory can we cut with this measurement while being conservative from a new physics perspective.

If the sensitivity is entirely driven by measuring the high p_T phase space region, the impact of operator mixing and running

[5] We use a modified version of [29] that includes the full numerical solution of the relevant RGEs. All scales are chosen $\mu = \sqrt{\hat{s}}$.

[6] Obviously this is the most conservative choice, and can be replaced by a statistically well-phrased criterion.

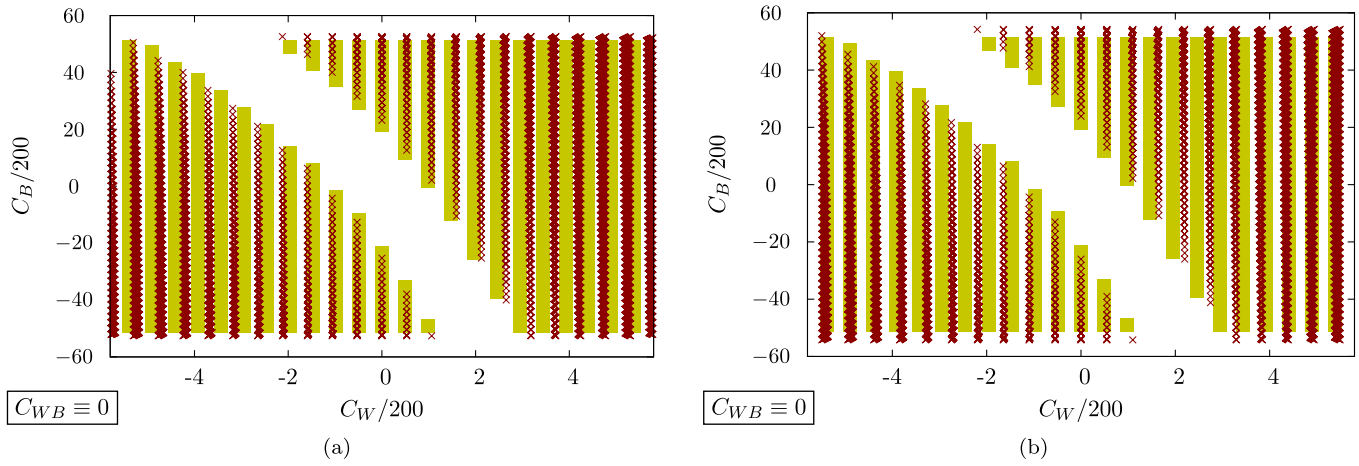

Fig. 6. (a) Scatter plot indicating the exclusion contours for $(C_W, C_B, C_{WB} = 0)$ from $pp \to HZ$ as detailed in the text. We choose $\Lambda_{\rm NP} \simeq 2.4$ TeV, which is the maximum energy scale probed in a toy MC experiment with statistics of $\mathcal{L} \simeq 1500/\text{fb}$ (only taking into account branching ratios $Z \to e^+e^-, \mu^+\mu^-$ and $H \to b\bar{b}$) following Section 3. (b) Same as (a) but choosing $\Lambda_{\rm NP} \simeq 14$ TeV, strictly outside the LHC 13 TeV coverage. To allow for direct a comparison we rescale the Wilson coefficients by $[14\ \text{TeV}/\max m_{\rm inv}]^2$ for (a).

becomes negligible. In binned log-likelihood hypothesis tests, a significant amount of sensitivity, however, also stems from lower p_T regions that are under better systematic and statistic control (we show a toy MC data sample in Fig. 5 for comparison).

Obviously, if we choose a cut-off of 14 TeV the impact is more pronounced. In most examples we chose 14 TeV, but we stress that this is a random choice at this stage, which is solely motivated by having an ad hoc EFT validity over the entire LHC run 2 energy range.

We compare $\Lambda_{\rm NP} = 14$ TeV with $\Lambda_{\rm NP} = m_{\rm inv}^{\rm max} \simeq 2.8$ TeV in Fig. 7 (for details see the caption). Since we only probe a single observable at this stage we have to make an assumption to reduce the numbers of parameters. We proceed as outlined in the preceding section to perform a measurement of $(C_W(\mu)), (C_B(\mu))$ subject to the boundary condition $C_{WB}(\mu) = 0$. Note that this is merely a choice to obtain an acceptable ρ parameter at this stage and C_{WB} can be constrained from other complementary measurements [34] (strictly speaking, the Z mass needs to be input as a boundary condition to the RGE running).

The difference between choosing $\Lambda_{\rm NP}$ outside the LHC coverage and as the maximum available energy is of course that the larger the ratio of $p_T/\Lambda_{\rm NP}$ becomes, the more important the deviation from the standard analysis that does not include the RGE running becomes.

Even though $C_{WB} = 0$ is a boundary condition at the measurement scale, operator running still induces $C_{WB} \neq 0$ at the UV scale. To give an estimate of numerical size, we show the induced exclusion contour in the (C_W, C_{WB}) plane for the $\Lambda_{\rm NP} = 14$ TeV in Fig. 7.

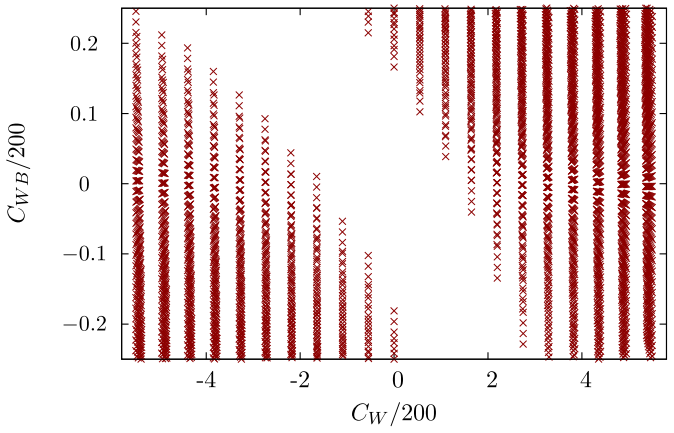

Fig. 7. Induced (C_W, C_{WB}) contour at the scale $\Lambda_{\rm NP}$ that results operator mixing of the scan shown in Fig. 6(b).

6. Conclusions

Coupling measurements at the 10% level can be obtained during the LHC run 2 [35]. This is the level of systematic uncertainty that can be expected from weak and strong operator running and mixing effects in the dimension 6 extension of the SM sector and other new physics scenarios as we have discussed using three instructive examples. Those particular examples comprehensively discuss the impact of QCD and electroweak operator mixing and running, especially for a class of phenomenologically highly relevant operators in the Higgs sector. As such they stand representative for other (possibly more complex) processes where we expect our findings to hold qualitatively as well. If the RGE-induced effects become of the order of the expected sensitivity, the resummation effects are relevant in reaching a consistent interpretation of new physics searches. We stress that there might well be additional sources of corrections of that size from additional one-loop effects.

A measurement of differential distributions constrains effective Lagrangians at different energy scales. These measurements can be consistently combined by using RGEs to evolve results to a well-defined and separated energy scale. We have outlined such a programme in Section 3.

For the discussed examples the impact of RGE running are of the order of $\lesssim$10%. If systematic uncertainties in specific channels turn out to be larger than this figure, our analysis demonstrates that the standard measurement approach that does not include any RGE running is perfectly adequate.

In case of systematic uncertainties being under sufficient control, we encourage the experiments to not only provide a numerical limit on Wilson coefficients as a result of their measurements, but in addition the distribution of a characteristic energy scale at which the operators have been probed as a consequence of our analysis. To give the measured constraint on the Wilson coefficients an interpretation in terms of a full UV theory requires to evolve the relevant coefficients to the theory-intrinsic cut-off scale. However, precisely this evolution depends on the shape of the differential distribution of the energy scale at which the operators have been probed during the measurement.

Our investigation was specific to the LHC run 2 where a vast range of energy scales will be probed in a fully differential fashion at high luminosity, but generalises straightforwardly to a future 100 TeV concept where the discussed phase space effects can be much larger, or a future linear collider where measurements at the percent-level will be possible.

Acknowledgements

We thank Céline Degrande for FeynRules support and Joachim Brod, Michael Spira and David Straub for helpful discussions. We thank Uli Nierste for very valuable comments on the manuscript.

C.E. thanks Cheikh Anta Diop University Dakar and the attendants and organisers of the African School of Fundamental Physics 2014, and the organisers of the ICTP GOAL workshop in São Paulo for the hospitality during the time when this work was completed. C.E. is supported by the IPPP, DU (grant number ST/G000905/1), Associateship programme.

M.S. thanks the Aspen Center for Physics for hospitality while part of this work was completed. This work was supported in part by the National Science Foundation under Grant No. PHYS-1066293.

References

[1] G. Aad, et al., ATLAS Collaboration, Phys. Lett. B 716 (2012) 1, arXiv:1207.7214 [hep-ex].
[2] S. Chatrchyan, et al., CMS Collaboration, Phys. Lett. B 716 (2012) 30, arXiv:1207.7235 [hep-ex].
[3] ATLAS Collaboration, ATLAS-CONF-2012-170;
CMS Collaboration, CMS-PAS-HIG-12-045.
[4] A. David, et al., LHC Higgs Cross Section Working Group Collaboration, arXiv:1209.0040 [hep-ph].
[5] K. Hagiwara, R.D. Peccei, D. Zeppenfeld, K. Hikasa, Nucl. Phys. B 282 (1987) 253.
[6] W. Buchmuller, D. Wyler, Nucl. Phys. B 268 (1986) 621.
[7] B. Grzadkowski, M. Iskrzynski, M. Misiak, J. Rosiek, J. High Energy Phys. 1010 (2010) 085, arXiv:1008.4884 [hep-ph].
[8] G.F. Giudice, C. Grojean, A. Pomarol, R. Rattazzi, J. High Energy Phys. 0706 (2007) 045, arXiv:hep-ph/0703164.
[9] P.J. Fox, C. Williams, Phys. Rev. D 87 (5) (2013) 054030, arXiv:1211.6390 [hep-ph];
O. Buchmueller, M.J. Dolan, C. McCabe, J. High Energy Phys. 1401 (2014) 025, arXiv:1308.6799 [hep-ph];
O. Buchmueller, M.J. Dolan, S.A. Malik, C. McCabe, arXiv:1407.8257 [hep-ph].
[10] C. Grojean, E.E. Jenkins, A.V. Manohar, M. Trott, J. High Energy Phys. 1304 (2013) 016, arXiv:1301.2588 [hep-ph].
[11] E.E. Jenkins, A.V. Manohar, M. Trott, J. High Energy Phys. 1310 (2013) 087, arXiv:1308.2627 [hep-ph];
E.E. Jenkins, A.V. Manohar, M. Trott, J. High Energy Phys. 1401 (2014) 035, arXiv:1310.4838 [hep-ph];
R. Alonso, E.E. Jenkins, A.V. Manohar, M. Trott, J. High Energy Phys. 1404 (2014) 159, arXiv:1312.2014 [hep-ph].
[12] J. Elias-Miro, J.R. Espinosa, E. Masso, A. Pomarol, J. High Energy Phys. 1311 (2013) 066, arXiv:1308.1879 [hep-ph].
[13] J. Ellis, V. Sanz, T. You, arXiv:1404.3667 [hep-ph].
[14] A. Biekoetter, A. Knochel, M. Kraemer, D. Liu, F. Riva, arXiv:1406.7320 [hep-ph].
[15] A. Pomarol, F. Riva, J. High Energy Phys. 1401 (2014) 151, arXiv:1308.2803 [hep-ph].
[16] B. Dumont, S. Fichet, G. von Gersdorff, J. High Energy Phys. 1307 (2013) 065, arXiv:1304.3369 [hep-ph].
[17] G. Buchalla, A.J. Buras, M.E. Lautenbacher, Rev. Mod. Phys. 68 (1996) 1125, arXiv:hep-ph/9512380.
[18] M.K. Gaillard, B.W. Lee, Phys. Rev. Lett. 33 (1974) 108;
F.J. Gilman, M.B. Wise, Phys. Rev. D 20 (1979) 2392;
G. Altarelli, G. Curci, G. Martinelli, S. Petrarca, Nucl. Phys. B 187 (1981) 461;
A.J. Buras, P.H. Weisz, Nucl. Phys. B 333 (1990) 66.
[19] U. Baur, E.W.N. Glover, Nucl. Phys. B 339 (1990) 38.
[20] R.V. Harlander, T. Neumann, Phys. Rev. D 88 (2013) 074015, arXiv:1308.2225 [hep-ph];
A. Banfi, A. Martin, V. Sanz, arXiv:1308.4771 [hep-ph];
A. Azatov, A. Paul, J. High Energy Phys. 1401 (2014) 014, arXiv:1309.5273 [hep-ph];
C. Grojean, E. Salvioni, M. Schlaffer, A. Weiler, J. High Energy Phys. 1405 (2014) 022, arXiv:1312.3317 [hep-ph];
M. Schlaffer, M. Spannowsky, M. Takeuchi, A. Weiler, C. Wymant, arXiv:1405.4295 [hep-ph];
M. Buschmann, C. Englert, D. Goncalves, T. Plehn, M. Spannowsky, Phys. Rev. D 90 (2014) 013010, arXiv:1405.7651 [hep-ph].
[21] J. Alwall, M. Herquet, F. Maltoni, O. Mattelaer, T. Stelzer, J. High Energy Phys. 1106 (2011) 128, arXiv:1106.0522 [hep-ph].
[22] C. Degrande, C. Duhr, B. Fuks, D. Grellscheid, O. Mattelaer, T. Reiter, Comput. Phys. Commun. 183 (2012) 1201, arXiv:1108.2040 [hep-ph].
[23] A. Alloul, N.D. Christensen, C. Degrande, C. Duhr, B. Fuks, Comput. Phys. Commun. 185 (2014) 2250, arXiv:1310.1921 [hep-ph].
[24] W.T. Giele, E.W.N. Glover, D.A. Kosower, Phys. Rev. Lett. 73 (1994) 2019, arXiv:hep-ph/9403347;
Z. Nagy, Phys. Rev. Lett. 88 (2002) 122003, arXiv:hep-ph/0110315;
Z. Nagy, Phys. Rev. D 68 (2003) 094002, arXiv:hep-ph/0307268;
S. Alioli, K. Hamilton, P. Nason, C. Oleari, E. Re, J. High Energy Phys. 1104 (2011) 081, arXiv:1012.3380 [hep-ph];
S. Dittmaier, A. Huss, C. Speckner, J. High Energy Phys. 1211 (2012) 095, arXiv:1210.0438 [hep-ph];
J. Currie, A. Gehrmann-De Ridder, E.W.N. Glover, J. Pires, J. High Energy Phys. 1401 (2014) 110, arXiv:1310.3993 [hep-ph].
[25] T. Aaltonen, et al., CDF Collaboration, Phys. Rev. D 78 (2008) 052006, arXiv:0807.2204 [hep-ex];
T. Aaltonen, et al., CDF Collaboration, Phys. Rev. D 79 (2009) 119902 (Erratum);
V.M. Abazov, et al., D0 Collaboration, Phys. Rev. Lett. 101 (2008) 062001, arXiv:0802.2400 [hep-ex];
G. Aad, et al., ATLAS Collaboration, Phys. Rev. D 86 (2012) 014022, arXiv:1112.6297 [hep-ex];
S. Chatrchyan, et al., CMS Collaboration, Phys. Lett. B 700 (2011) 187, arXiv:1104.1693 [hep-ex].
[26] C. Englert, J. Jaeckel, E. Re, M. Spannowsky, Phys. Rev. D 85 (2012) 035008, arXiv:1111.1719 [hep-ph];
Y. Bai, P. Draper, J. Shelton, J. High Energy Phys. 1207 (2012) 192, arXiv:1112.4496 [hep-ph];
A. Djouadi, A. Falkowski, Y. Mambrini, J. Quevillon, Eur. Phys. J. C 73 (2013) 2455, arXiv:1205.3169 [hep-ph].
[27] T. Hahn, Comput. Phys. Commun. 140 (2001) 418, arXiv:hep-ph/0012260;
T. Hahn, M. Perez-Victoria, Comput. Phys. Commun. 118 (1999) 153, arXiv:hep-ph/9807565.
[28] K. Fujikawa, B.W. Lee, A.I. Sanda, Phys. Rev. D 6 (1972) 2923.
[29] J. Baglio, J. Bellm, F. Campanario, B. Feigl, J. Frank, T. Figy, M. Kerner, L.D. Ninh, et al., arXiv:1404.3940 [hep-ph];
K. Arnold, M. Bahr, G. Bozzi, F. Campanario, C. Englert, T. Figy, N. Greiner, C. Hackstein, et al., Comput. Phys. Commun. 180 (2009) 1661, arXiv:0811.4559 [hep-ph].
[30] J.M. Campbell, R.K. Ellis, R. Frederix, P. Nason, C. Oleari, C. Williams, J. High Energy Phys. 1207 (2012) 092, arXiv:1202.5475 [hep-ph];
X. Liu, F. Petriello, Phys. Rev. D 87 (9) (2013) 094027, arXiv:1303.4405 [hep-ph];
R. Boughezal, F. Caola, K. Melnikov, F. Petriello, M. Schulze, J. High Energy Phys. 1306 (2013) 072, arXiv:1302.6216 [hep-ph].
[31] J.M. Butterworth, A.R. Davison, M. Rubin, G.P. Salam, Phys. Rev. Lett. 100 (2008) 242001, arXiv:0802.2470 [hep-ph];
D.E. Soper, M. Spannowsky, J. High Energy Phys. 1008 (2010) 029, arXiv:1005.0417 [hep-ph].
[32] G. Isidori, M. Trott, J. High Energy Phys. 1402 (2014) 082, arXiv:1307.4051 [hep-ph].
[33] R.V. Harlander, S. Liebler, T. Zirke, J. High Energy Phys. 1402 (2014) 023, arXiv:1307.8122 [hep-ph];
C. Englert, M. McCullough, M. Spannowsky, Phys. Rev. D 89 (2014) 013013, arXiv:1310.4828 [hep-ph].
[34] R. Contino, M. Ghezzi, C. Grojean, M. Muhlleitner, M. Spira, J. High Energy Phys. 1307 (2013) 035, arXiv:1303.3876 [hep-ph].
[35] C. Englert, A. Freitas, M. Muhlleitner, T. Plehn, M. Rauch, M. Spira, K. Walz, arXiv:1403.7191 [hep-ph].